DOI: 10.1002/smll.200700211

# Stable, High-Efficiency Ionic-Liquid-Based Mesoscopic Dye-Sensitized Solar Cells

*Daibin Kuang, Cedric Klein, Zhipan Zhang, Seigo Ito, Jacques-E. Moser, Shaik. M. Zakeeruddin,* and Michael Grätzel**

***E**fficient and stable mesoscopic dye-sensitized solar cells (DSCs) introducing a low-viscosity binary ionic liquid (1-propyl-3-methyl-imidazolium iodide (PMII) and 1-ethyl-3-methyl-imidazolium tetracyanoborate ($EMIB(CN)_4$)) electrolyte in combination with a new high-molar-extinction-coefficient ruthenium complex, Ru(2,2′-bipyridine-4,4′-dicarboxylic acid)(4,4′-bis(2-(4-tert-butyloxy -phenyl)ethenyl) −2,2′-bipyridine) $(NCS)_2$, are demonstrated. The dependence of photovoltaic performance, charge transport and electron lifetime on the composition of the binary ionic-liquid electrolyte with different ratios of PMII/$EMIB(CN)_4$ were investigated by electrochemical impedance and photovoltage transient techniques. A photovoltaic conversion efficiency of 7.6 % was obtained under simulated full sunlight illumination, which is a record for solvent-free DSCs. These devices exhibit excellent stability at 80 °C in the dark or under visible-light soaking at 60 °C during 1000 h of accelerated tests.*

**Keywords:**
- dyes
- ionic liquids
- nanocrystals
- solar cells

## 1. Introduction

Mesoscopic dye-sensitized solar cells (DSCs) have attracted intense interest owing to the prospect of cheap, efficient light-to-electricity power conversion.[1–3] For high performance, fast electron injection from the excited state of the dye into the $TiO_2$ film, rapid dye regeneration, slow electron recombination at the $TiO_2$–electrolyte interface as well as efficient charge-carrier collection by fast electron diffusion in the mesospic $TiO_2$ film and transport of the redox mediator in the electrolyte are crucial.[4–6] Record efficiencies exceeding 11 % under standard AM 1.5 solar illumination have been reached with volatile electrolytes[6d,7,8] having a boiling point near 100 °C. However, due to their high vapour pressure, they are difficult to use outdoors in warm climates; hermetic sealing requirements pose a challenge for practical application. In the last decade, much attention has therefore been paid to the development of nonvolatile electrolytes meeting the stability requirements for outdoor applications.[9] In parallel, a series of high-molar-extinction-coefficient ruthenium complexes containing π-conjugated ligand systems have been successfully introduced and have shown excellent photovoltaic performance and stability.[6,10] Employing these new sensitizers in conjunction with a nonvolatile electrolyte has recently culminated in the realization of a >9 % efficient DSC exhibiting excellent stability under light soaking and thermal stress.[6d] However, this electrolyte still contains an organic solvent, that is, methoxypropionitrile (MPN), which precludes important applications for lightweight and flexible photovoltaic (PV) devices due to MPN permeation across the plastic current collector. The ultimate redox electrolyte for universal employment in the DSC should be solvent free.

[*] Dr. D. Kuang, Dr. C. Klein, Z. Zhang, Dr. S. Ito, Prof. J.-E. Moser, Dr. S. M. Zakeeruddin, Prof. M. Grätzel
Laboratory for Photonics and Interfaces
Institute of Chemical Sciences and Engineering
Ecole Polytechnique Fédérale de Lausanne
1015 Lausanne, Switzerland
Fax: (+41) 21-6934111
E-mail: shaik.zakeer@epfl.ch
michael.graetzel@epfl.ch

NANO MICRO small

Ionic liquids (ILs) represent a new and attractive class of solvent-free electrolytes, having some characteristics of molten salts. Recently synthesized compounds are moisture, air, and temperature stable. They have a high conductivity and a very wide (>4 V) electrochemical stability window. Their melting points are distinctly below room temperature. Importantly, they have no detectable vapour pressure even at the elevated operating temperatures of PV cells, presenting a huge practical advantage over all organic-solvent electrolytes including the nonvolatile "super robust" formulation introduced recently.[6d] A number of ILs have already been examined for DSCs.[6a,11–15] However, till recently their performance lagged so far behind that of the organic solvent-based systems that the realm of applications was believed to be restricted to indoor applications where low light levels prevail.[16]

Until now ILs using imidazolium cations have fared the best for the DSC, but if iodide and triiodide are the only counter ions present, their viscosity becomes several hundred mPas, imposing severe mass-transfer limitations on the photocurrent in full sunlight. The very high concentration (ca 5.8 M) of $I^-$ present in the pure imidazolium iodide melts entails two other disadvantages, the first being a reduction of the open circuit voltage ($V_{oc}$) of the cell due to the lowering of the Nernst potential of the counter-electrode and the second the occurrence of reductive quenching of the ruthenium sensitizer competing with electron injection from the excited state and decreasing the short-circuit photocurrent density ($J_{sc}$) of the cell.[17] These problems are alleviated by adding a low-viscosity IL having an inert anion to the iodide-containing IL. A variety of such binary ILs containing different anions have been explored, such as bis(trifluoromethylsulfonyl) imide ($Tf_2N^-$), thiocyanate ($NCS^-$), tricyanomethanide ($C(CN)_3^-$) and tetracyanoborate ($B(CN)_4^-$).[6a,11,16,17] Of those, only $Tf_2N^-$ and the newly developed $B(CN)_4^-$ have shown stable performance in the DSC, but the $EMIB(CN)_4$, whose viscosity is only 19.8 cP at 20 °C, has shown particular promise[11] warranting further investigation. In this Full Paper, we report on a new record 7.6% power-conversion efficiency under AM 1.5 full sun irradiation using a $EMIB(CN)_4$-based binary IL in combination with the high-molar-extinction-coefficient sensitizer (K77).

The results are compared with the performance of a DSC using the same sensitizer but an MPN-based organic-solvent electrolyte.[6d] Electrochemical impedance spectroscopy (EIS) and photovoltage transient measurements provide important and direct information on the performance of the critical circuit elements of this new DSC embodiment during light soaking and heat stress.

## 2. Results and Discussion

The ligand 4,4′-bis(2-(4-tert-butyloxyphenyl)ethenyl)-2,2′-bipyridine and the K77 dye were synthesized as shown in Scheme 1. The detailed synthetic procedure is reported elsewhere.[6d] The molecular structure of Ru(2,2′-bipyridine-4,4′-dicarboxylicacid)(4,4′-bis(2-(4-tert-butyloxyphenyl)ethenyl) −2,2′-bipyridine) $(NCS)_2$, coded as K77, is shown in Figure 1. The molar extinction coefficient for the lowest metal-to-ligand charge-transfer (MLCT) absorption band at 546 nm is of $19.4\times10^3\,M^{-1}\,cm^{-1}$, which is 1.5 times higher than that of the conventional Z907 dye.

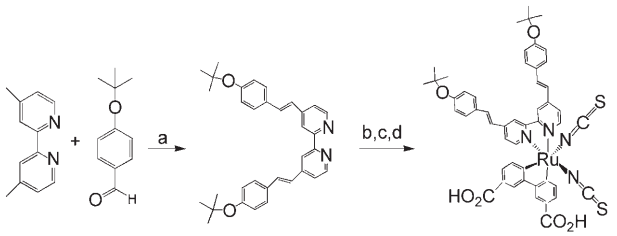


**Scheme 1.** Synthesis of K77. a) *t*BuOK, DMF, 25 °C. b) $[Ru(Cl)_2(p\text{-cymene})]_2$, EtOH, Δ. c) 4,4′-dicarboxy-2,2′-bipyridine, DMF, 140 °C. d) $NH_4NCS$, DMF, 140 °C.

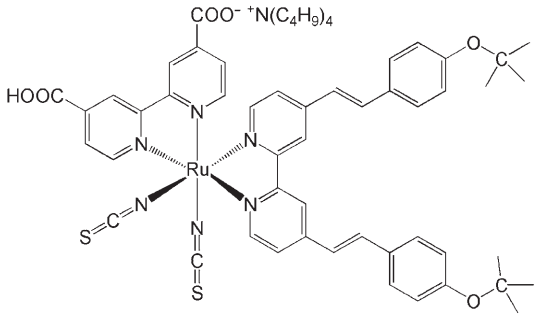


**Figure 1.** Molecular structure of the K77 sensitizer.

Since the photovoltaic performance of the dye-sensitized solar cells is largely dependent on the kinetic competition between back-electron transfer of the injected electrons from the conduction band of the semiconductor electrode to the oxidized dye cations ($S^+$) and the interception of the oxidized sensitizer by the redox mediator (dye regeneration), nanosecond time-resolved laser transient absorbance measurements were performed to scrutinize the kinetics of these two charge-transfer processes for the K77 dye in the presence of an inert IL or the $I^-/I_3^-$ ionic redox couple. Great care was taken to keep the excitation laser pulse intensity as low as possible (fluence $<20\,\mu J\,cm^{-2}$) in order to ensure that, at most, one electron was injected during one pulse per $TiO_2$ nanoparticle. The probe light intensity was also reduced to a minimum by use of filters and a monochromator placed before the sample in order to avoid light biasing of the sensitized $TiO_2$ films. In the electrochemically inert ionic liquid EMITFSI, the decay of the absorption signal recorded at $\lambda=680$ nm reflects the dynamics of the recombination of injected electrons with the oxidized dye ($S^+$). At the low laser-light intensities employed, the reaction involves only one geminate electron per $S^+$ pair occupying the same $TiO_2$ particle, hence it should follow first-order kinetics if the interfacial electron-transfer step and not the transport within the $TiO_2$ is rate determining.[18] This appears to be the case here as the rate data in the inert IL

  

could be fitted by a single exponential with a typical halflife $\tau_{1/2}=250\,\mu s$ yielding a rate constant of $k_b=1.6\times10^3\,s^{-1}$ (Figure 2). This value is 2.3 times smaller than the recombination rate constant of $3.7\times10^3\,s^{-1}$ measured in the MPN

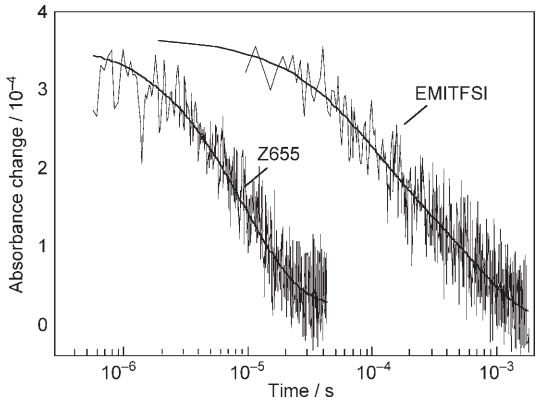


**Figure 2.** Transient absorbance decay kinetics of the oxidized state of K77 dye adsorbed on nanocrystalline $TiO_2$ films in EMITFSI redox-inactive IL and in Z655 electrolyte. Smooth solid lines are single exponential fits of experimental data. Absorbance changes were measured at a probe wavelength of 650 nm upon 600-nm pulsed-laser excitation (5 ns full width half-maximum pulse duration, 20 $\mu J\,cm^{-2}$ pulse fluence, 30 Hz repetition rate). Signals shown were obtained by typically averaging over 3000 laser shots.

solvent.[6d] The Marcus model for nonadiabatic electron-transfer reactions is normally employed to analyze the recapture dynamics of $TiO_2$ conduction-band electrons by the oxidized sensitizer.[19] Due to their large driving force and small reorganization energy these reactions fall in the inverted Marcus region. The recombination rate was found to be remarkably insensitive to the nature of ambient that surrounds the sensitizer.[19] More recent time-resolved studies carried out with a number of organic electrolytes under similar conditions as in the present investigation, that is, low laser intensities and absence of forward biasing of the dye-sensitized $TiO_2$ films, have confirmed the kinetics of recombination to be independent of electrolyte composition.[20] Solvent reorganization therefore does not appear to influence the electron-transfer dynamics to any significant extent. However, for ionic liquids the situation is special as the outer-sphere solvent reorganization energy is zero.[21] Thus, in the case of the IL, only the inner-sphere reorganization energy makes a contribution, which is very small for surface-adsorbed ruthenium complexes.[22] This shifts the reaction activation energy further in the inverted region, explaining why the recombination rate is lower for the IL than for MPN.

In the iodide-containing binary IL electrolyte, coded Z655, the decay of the oxidized dye signal was significantly accelerated, the halflife being $\tau_{1/2}=9\,\mu s$. The interception reaction is known to be pseudo first order with respect to iodide concentration.[23] Data could therefore be fitted to a single exponential yielding a rate constant of $k_r=1.0\times10^5\,s^{-1}$ for the pseudo first-order rate constant of the dye-regeneration process. The $k_r/k_b$ branching ratio of 62.5 indicates that 98.4% of oxidized dye is intercepted by electron donation from $I^-$ resulting in very efficient dye regeneration. For the MPN-based Z646 electrolyte[6d] the interception of the back reaction occurred with the same rate constant of $k_r=1.0\times10^5\,s^{-1}$ corresponding to a $k_r/k_b$ branching ratio of 27 and a 96.4% yield for dye regeneration. The agreement between the two $k_r$ values is fortuitous as the IL has a 3.5 times higher iodide concentration than the MPN-based organic electrolyte. The increased $I^-$ concentration appears to compensate slower mass transport in the IL, resulting in very similar interception rates. Thus for both electrolytes the dye-regeneration efficiency is close to unity.

The volume ratio of PMII/EMIB(CN)$_4$ in the binary IL electrolytes was optimized, maintaining 0.1 M Guanidinium thiocyanate (GuNCS), 0.2 M $I_2$ and 0.5 M N-methyl-benzimidazole (NMB) concentration in the IL mixtures containing different volume ratios of PMII and EMIB(CN)$_4$. The short-circuit current density ($J_{sc}$) and power-conversion efficiency ($\eta$) increases first when the PMII fraction is raised from 20% to 65%, as shown in Figure 3. Further increase in the PMII concentration reduces the $J_{sc}$ and $\eta$ values. A complete set of photovoltaic parameters for the different volume ratios is shown in Table 1.

The short-circuit current densities under AM 1.5 sun illumination for PMII volume percentages of 20, 65, and 100% are 9.5, 14.56, and 13.42 $mA\,cm^{-2}$, respectively. The corresponding photovoltaic efficiencies are 4.98%, 7.2%, and 6.4%, respectively, the changes in the open-circuit voltage ($V_{oc}$) and the fill factor (FF) being only a few percent.

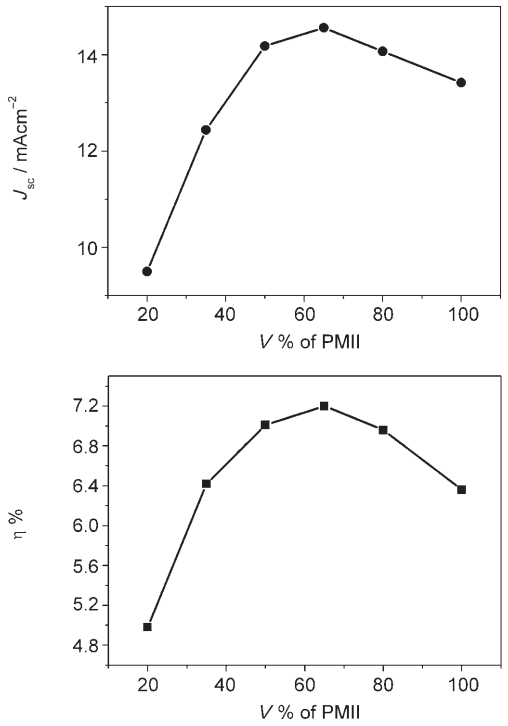


**Figure 3.** The short-circuit current density and photovoltaic efficiency of DSCs under AM 1.5 sunlight (100 $mW\,cm^{-2}$) as a function of the volume percentage of PMII in the binary IL containing EMIB(CN)4 as second component.

NANO MICRO small

**Table 1.** Complete set of photovoltaic parameters for DSCs based on K77 sensitizer and the binary IL electrolyte with various PMII volume percent measured under AM 1.5 full sunlight (100 mW cm$^{-2}$) irradiation.[a]

| PMII % | $J_{sc}$ [mA cm$^{-2}$] | $V_{oc}$ [mV] | FF | $H$ [%] |
|---|---|---|---|---|
| 100 | 13.42 | 0.700 | 0.677 | 6.4 |
| 80 | 14.07 | 0.709 | 0.698 | 7 |
| 65 | 14.56 | 0.709 | 0.697 | 7.2 |
| 50 | 14.18 | 0.713 | 0.693 | 7.01 |
| 35 | 12.44 | 0.714 | 0.723 | 6.42 |
| 20 | 9.5 | 0.707 | 0.725 | 4.98 |

[a] The spectral distribution of the xenon lamp simulates AM 1.5 solar light. The active area of the devices with a metal mask is 0.158 cm$^{-2}$.

The best results are obtained using a PMII/EMIB(CN)$_4$ of 65 %/35 %.

Figure 4 shows the photocurrent dynamics for various volume percentages of PMII and different light intensity.

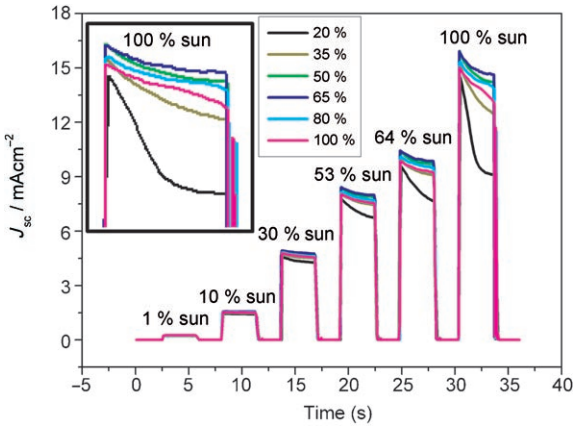


**Figure 4.** Current dynamics of DSCs based on K77 sensitizer and the binary IL electrolytes with different volume percentage of PMII under various light intensities. The inset shows the enlarged part for 100 % sun light.

The short-circuit photocurrent is shown in response to a light on–off sequence produced by opening and closing a mechanical shutter that blocks the light beam. Under low light levels ($<100$ W m$^{-2}$), the photocurrent signal raises vertically to remain constant on a time scale of seconds while for all PMII concentrations a decay is noted when the light intensity passes 300 W m$^{-2}$. The relative decay in the photocurrent depends on the IL composition and increases with increasing light intensity, indicating control of the photocurrent by mass transfer under these conditions. For DSCs based on low-viscosity organic-solvent electrolytes such as acetonitrile or the recently described MPN-based formulation,[6d] no current decay is observed even under full sunlight illumination as there is no mass-transport limitation. Note that the IL containing 20 % PMII showed the largest photocurrent transient even though it has the lowest viscosity. This is attributed to a lack of dye regeneration due to the $I^-$ depletion in the pores. However, for 100 % PMII (5.8 M of $I^-$), a linear decay of photocurrent was observed due to the mass-transport limitation because of the high viscosity of electrolyte. Figure 4 shows that DSCs based on the binary IL electrolyte containing 65 % PMII in volume percent have only 8 % photocurrent decay at full sun irradiation, the smallest fraction for all examined compositions. The mass-transport limitation of the $J_{sc}$ in full sunlight accounts for the remaining relatively small difference in the conversion efficiency (7–8 %) achieved with the new IL-based DSC and that of the MPN based organic electrolyte (8–9 %).[6d] The present results are very encouraging pointing at future opportunities to further enhance the performance of this very important solvent-free DSC system.

For further analysis the diffusion coefficients of $I^-$ and $I_3^-$ were measured (Table 2) at various concentrations of PMII in the binary ILs. The diffusion coefficient of $I^-$ and $I_3^-$ were obtained from the anodic and cathodic steady-state currents ($I_{ss}$) according to the equation[24] $I_{ss}=4ncaFD_{app}$, where $a$ is the microelectrode radius, $n$ is the number of electrons transferred in the electrochemical step, $F$ is the Faraday constant and $c$ is the bulk concentration of electroactive species. The diffusion coefficients of $I^-$ and $I_3^-$ decreased from $6.03\times10^{-7}$ to $3.93\times10^{-7}$ cm$^2$ s$^{-1}$ and $7.18\times10^{-7}$ to $2.03\times10^{-7}$ cm$^2$ s$^{-1}$, respectively, with PMII concentration increasing from 20 % to 100 %.

**Table 2.** Diffusion coefficients of iodide and triiodide for ILs based on different volume percentages of PMII.

| PMII % (vol) | $D_{I^-}$ [$10^{-7}$ cm$^2$ s$^{-1}$][a] | $D_{I3^-}$ [$10^{-7}$ cm$^2$ s$^{-1}$][a] | $D_{I3^-}$ [$10^{-7}$ cm$^2$ s$^{-1}$][b] |
|---|---|---|---|
| 20 % | 6.03 | 7.18 | 5.50 |
| 35 % | 5.75 | 5.86 | 4.94 |
| 50 % | 5.04 | 4.64 | 4.83 |
| 65 % | 4.3 | 3.51 | 3.81 |
| 80 % | 4.4 | 2.65 | 2.64 |
| 100 % | 3.93 | 2.03 | 2.36 |

[a] Calculated from microelectrode measurements and [b] obtained from the EIS measurements.

  

DSC devices fabricated by K77 dye in the presence of 3-phenylpropionic acid (PPA) as co-adsorbent, using the binary IL containing 65% of PMII and 35% of $EMIB(CN)_4$, resulted in the highest efficiency of 7.6% under full sunlight illumination. Figure 5a presents the photocurrent-density–voltage curves of the DSC measured

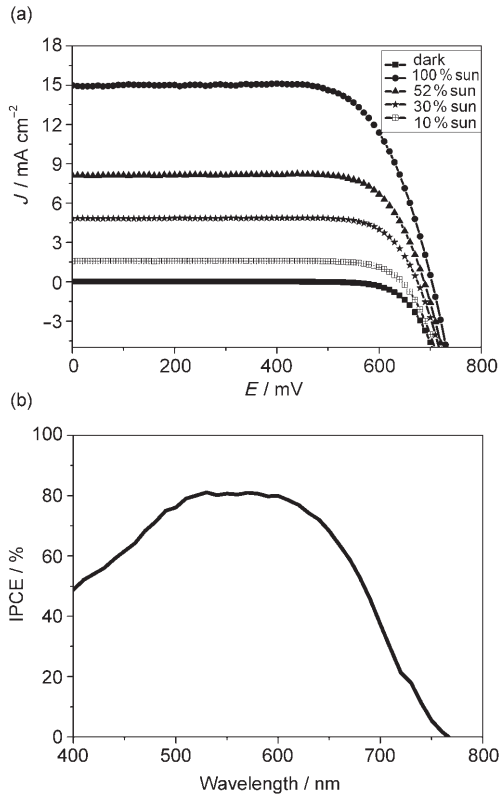


**Figure 5.** a) *I–V* curves of DSCs based on K77 sensitizer with PPA co-adsorbant and the binary IL electrolyte using the optimal volume ratio of PMII/$EMIB(CN)_4$, namely 65% of PMII and 35% of $EMIB(CN)_4$, measured under different light-intensity irradiations. b) Photocurrent action spectrum of the above device. The active area of the device with a metal mask is 0.158 cm$^2$.

under various light-intensity irradiations. The short-circuit current density ($J_{sc}$), open-circuit voltage ($V_{oc}$), and fill factor (FF) under simulated AM 1.5 illumination were 15.1 mA cm$^{-2}$, 702 mV, and 0.714, respectively. It is interesting to note that 8.6% power-conversion efficiency was obtained under one third of a sun (300 W m$^{-2}$). The incident photon-to-current conversion efficiency (IPCE) defined as the number of generated electrons divided by the number of incident photons is shown in Figure 5b. The IPCE spectrum reveals that the maximal efficiency was over 80% at 546 nm and exceeds 70% in spectral range between 480 nm and 650 nm.

Electrochemical impedance spectroscopy (EIS) is a powerful technique for characterization of electronic or ionic transport process in DSCs.[6a,11,25] . The different volume ratios of PMII/$EMIB(CN)_4$ were therefore subjected to EIS investigation. Figure 6 shows the impedance data measured in darkness under −0.7 V applied bias. Three typical characterization frequency peaks in the Bode phase plots (Figure 6a) or three typical semicircles in the Nyquist plots (Figure 6b) are observed, which correspond to the $I_3^-$ transport in the electrolyte, electron recombination at the $TiO_2$/electrolyte interface together with electron transport in the $TiO_2$ network, and charge transfer at the counter electrode in the order of increasing frequency. Using the equation $D = L^2/\tau_d$, one derives from the fitted $\tau_d$ of the lower frequency arc in Figure 6b, diffusion coefficients of triiodide for the electrolyte with different PMII concentration are shown in Table 2. The low-frequency peak position value decreases with increasing PMII volume percent in keeping with the decrease in the $I_3^-$ diffusion coefficient from $5.5\times10^{-7}$ to $2.36\times10^{-7}$ cm$^2$ s$^{-1}$. The middle peak shifts to higher frequency with increasing PMII content implying a slight decrease in the electron lifetime. This can be ascribed to enhanced electron recombination with $I_3^-$ due to the augmentation of the viscosity causing slower evacuation of the $I_3^-$ from the pores. The electron lifetime of 20%, 65%, and 100% PMII containing IL are 18.8 ms, 16.5 ms and 15.5 ms, respectively, which were obtained by using appropriate equivalent circuits to fit the impedance spectra. The high-frequency peak reflects the $I_3^-$ reduction time at the counter electrode. It shifts to lower values upon increasing the PMII mole fraction, revealing the slower electron transfer at the counter electrode because of higher viscosity and slower diffusion of $I_3^-$. This explains why the fill factor decreases at higher PMII concentration. Thus the EIS measurements for DSCs based on various volume ratio of PMII/$EMIB(CN)_4$ electrolytes is consistent with the above photovoltaic data.

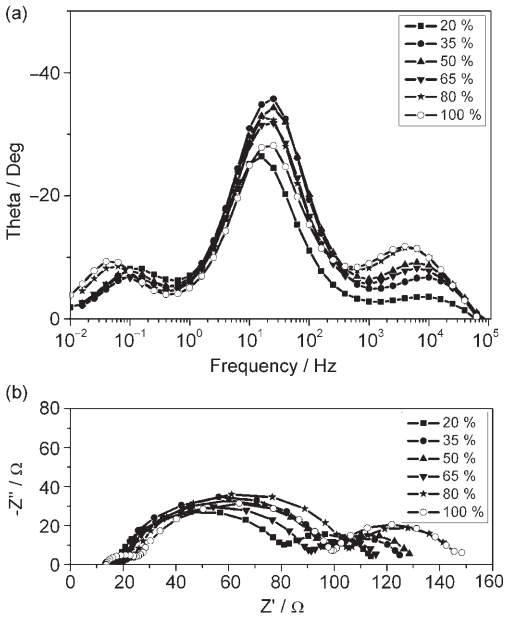


**Figure 6.** Impedance spectra of DSCs based on K77 sensitizer and the binary IL electrolytes with different volume percentage of PMII, measured in darkness under −0.70 V applied bias. a) Bode phase plots, b) Nyquist plots.

A photovoltage transient decay study was performed to assess the electron-lifetime dependence on the PMII content in the binary PMII/$EMIB(CN)_4$ ILs. Results obtained

  

NANO MICRO small

at different open-circuit potentials ($V_{oc}$) are shown in Figure 7. The $V_{oc}$ was adjusted by varying the light bias level. The electron lifetime decreases with the PMII volume fraction, values at 20%, 65% and 100% being 7.2 ms,

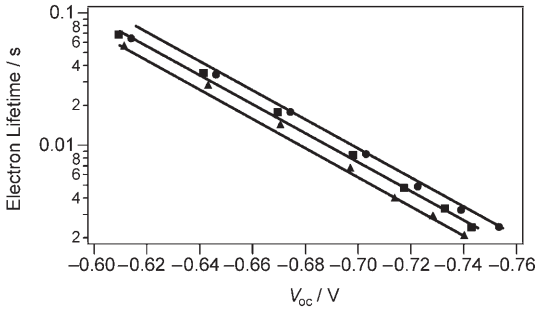


**Figure 7.** Electron lifetimes of the devices based on K77 sensitizer and IL with different volume ratio of PMII/EMIB(CN)$_4$ at open-circuit voltage under varying light bias. Dot curve: PMII/EMIB(CN)$_4$ is 20:80, square: PMII/EMIB(CN)$_4$ is 65:35, triangle: 100% PMII.

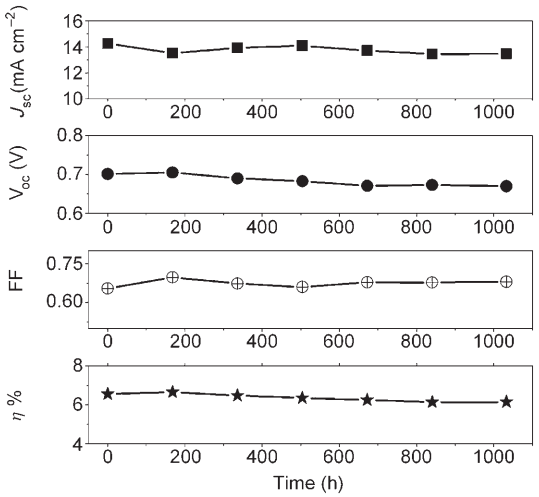


**Figure 8.** Time dependence of photovoltaic parameters ($J_{sc}$, $V_{oc}$, FF, and $\eta$) of DSCs based on K77 sensitizer and the binary IL electrolyte varied with the time during the accelerated tests at 80 °C in darkness.

5.8 ms and 5.3 ms under one sun illumination, respectively. The same tendency was observed in the EIS measurements. Clearly, the presence of tetracyanoborate instead of iodide at the interface retards the recapture of conduction-band electrons by triiodide ions. A likely reason for this effect is the coordination of surface titanium ions by cyanide groups reducing the density of states that act as recombination center. The earlier observation that binary ILs containing dicyanoamide and tricyanomethide counter ions show higher $V_{oc}$ values than the pure iodide melts supports this interpretation.

It was noted that the absolute values of the electron lifetimes observed from photovoltage transient measurements at a specific concentration of PMII were smaller than those derived from the EIS measurements. This behaviour can be rationalized in terms of different local $I_3^-$ concentrations present in the pores of the nanocrystalline titania film. During the photovoltage transient decay studies the DSC is illuminated leading to a higher $I_3^-$ concentration than in the EIS experiments that were conducted in the dark.

Accelerated aging tests were performed to scrutinize the photo and thermal stability of the new solvent-free DSC system employing the EMIB(CN)$_4$-based binary IL along with the K77 sensitizer. The Z655 electrolyte contained 0.1 M GuNCS, 0.2 M $I_2$ and 0.5 M NBB in a 65/35 v/v% mixture of PMII/EMIB(CN)$_4$ . Figure 8 presents the photovoltaic data of the DSC during aging at 80 °C in the dark. The performance was remarkably stable over this period a 30 mV $V_{oc}$ decay and 0.7 mA cm$^{-2}$ decrease of $J_{sc}$ being compensated by an increase in FF (5%). Hence, 91% of the initial photovoltaic performance was retained even after a continuous 1000 h accelerated test under above conditions. The cells maintained more than 90% of their initial efficiency under light soaking at 60 °C for 1000 h confirming that the stability is similar to that of the MPN-based organic electrolyte. The fill factors are high for both types of electrolyte attaining more than 70 percent during the aging experiments. In view of the much higher viscosity of the IL compared to the MPN-based liquid the high FF value obtained with the former is remarkable. One would have expected the fill factor of the IL cell to suffer from the diffusion-limited transfer of triiodide ions to the counter electrode. It appears, however, that this is compensated by the very effective and rapid charge screening achieved in the IL assisting in the photoinduced charge separation and avoiding losses that occur in the MPN-based electrolyte due to ion pairing.

EIS studies were performed with fresh and aged devices to explain the variations in the photovoltaic performances during aging time. Figure 9 shows the impedance spectroscopy of the initial cell and aged cell after 1000 h accelerated test under 80 °C in darkness. Indications of photovoltage and efficiency decrease can be seen since the middle frequency peak shifts to a slightly higher frequency in the Bode phase plots, which means that the electron lifetime decreased for the aged cell. The calculated values of the elec-

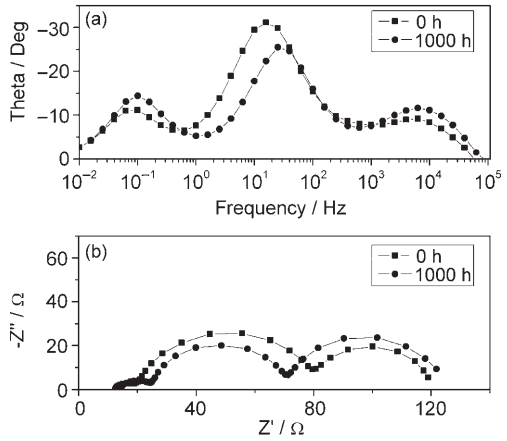


**Figure 9.** Impedance spectra of DSCs based on K77 and the binary IL electrolyte (Z655) for the fresh and aged cell following the accelerated testing time (1000 h) at 80 °C in darkness, measured as −0.7 V bias. a) Bode phase plots, b) Nyquist plots.

  

tron lifetime according to the appropriate equivalent circuit are 20.9 ms and 9.6 ms for fresh cell and aged cell, respectively. Interestingly, this decrease is smaller than that observed with the MPN-based electrolyte where the electron lifetime decreased from 62.5 to 15.2 ms during thermal aging.[6d] Further studies are under way to elucidate this observation.

The high-frequency peak also shifts to larger values, implying faster electron transfer at the counter electrode for the aged cell, which will result in an improved fill factor in agreement with the photovoltaic data. The increase in the radius of the low-frequency hemicycle in the Nyquist plot shows that the diffusion resistance augments during aging probably due to a decrease in the triiodide concentration caused by reaction with impurities.[11]

Photovoltage transient measurements were performed on the DSC devices to investigate the variation of electron lifetime for the fresh and aged cells. Figure 10 presents the electron lifetimes at open-circuit conditions under various

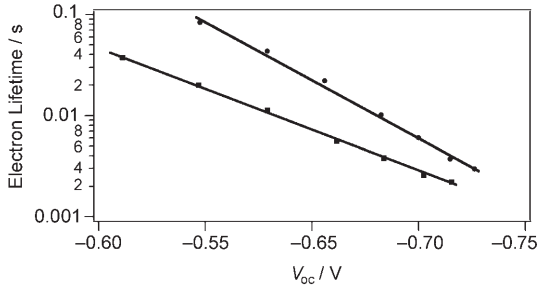


**Figure 10.** Electron lifetimes of the fresh and aged devices (after 1000 h accelerated testing at 80 °C in darkness) at open-circuit voltage under varying light bias. Dot curve: fresh cell, square curve: aged cell.

light bias levels for fresh and aged cells. The electron lifetime of DSCs are 6.1 ms and 4.7 ms at the corresponding open-circuit voltage for the initial cell and aged cell, respectively. Both EIS and photovoltage transient results confirm the electron-lifetime decrease during the aging is responsible for the photovoltage and photovoltaic performance decay. It is interesting to note that the absolute value of electron lifetime from EIS is larger than that of electron lifetime from photovoltage transient measurements, which is probably due to different measurement conditions. EIS measurements were performed in darkness and therefore with a lower $I_3^-$ concentration around the $TiO_2$ electrode compared to the photovoltage transient measurements that were measured under light illumination resulting in higher $I_3^-$ concentration. Hence short electron lifetime can be observed for the latter measurement.

## 3. Conclusions

For the first time, a 7.6% photon-to-electricity conversion efficiency was reached with a solvent-free DSC using the PMII/EMIB(CN)$_4$ binary IL in conjunction with the new high-molar-extinction-coefficient sensitizer (K77). The effects of volume ratio on the photovoltaic performance were investigated and the optimal volume ratio was 65%:35%.The photovoltaic parameters ($J_{sc}$, $V_{oc}$, FF, and $\eta$) with various PMII fractions were evaluated by electrochemical impedance spectroscopy and photovoltage transient techniques. EIS results reveal that the $I_3^-$ transport in the electrolyte and charge transfer at the counter electrode become slower with the increasing PMII concentration due to the increase in viscosity of the binary IL electrolyte. Both EIS and photovoltage transient measurements show that the electron lifetime of DSCs decreases after a 1000 h accelerated test at 80 °C in darkness. The present results are very encouraging pointing at future opportunities to further enhance the performance of this very important solvent-free DSC system.

## 4. Experimental Section

*Reagents*: The high-molar-extinction-coefficient sensitizer K77, Ru(2,2′-bipyridine-4,4′-dicarboxylic acid)(4,4′-bis(2-(4-tert-butyloxyphenyl)ethenyl) -2,2-bipyridine) $(NCS)_2$ and 1-butyl-1H-benzimidazole (NBB) were synthesized as reported earlier.[6d] The ILs 1-propyl-3-methylimidazolium iodide (PMII), 1-ethyl-3-methylimidazolium bis(trifluoromethylsulfonyl)imide (EMITFSI), and 1-ethyl-3-methyl-imidazolium tetracyanoborate (EMIB(CN)$_4$) were synthesized according to the literature methods and the purity was confirmed by $^1$H NMR analysis.[16,26] 3-phenylpropionic acid (PPA) and guanidinium thiocyanate (GuNCS) was purchased from Aldrich. N-methylbenzimidazole (NMB, from Aldrich) was recrystallized from diethyl ether before use. N-butyl-benzimidazole (NBB) was synthesized according to the literature method.[6d]

*EIS*: Impedance spectra of DSCs were measured in the dark at −0.7 V forward bias using a potentiostat (EG&G, M273) equipped with a frequency-response analyzer (EG&G, M1025). The spectra were scanned in a frequency range of 0.005 Hz ≈100 kHz at room temperature with modulation amplitude set at 10 mV. The obtained impedance spectra were fitted with Z-View software (v2.8b, Scribner Associates Inc.) to the appropriated equivalent circuits.[25]

*Diffusion coefficient measurements*: A two-electrode electrochemical cell, consisting of a 5.0-μm-radius Pt ultramicroelectrode as working electrode and a Pt foil as counter electrode, was used to measure the iodide and triiodide diffusion coefficient. The radius of the Pt microelectrode was determined by using standard solutions.

*Photovoltage transient decay*: Photovoltage transients were measured using a pump pulse generated by a ring of red LEDs controlled by a fast solid-state switch. Pulse widths of 200 ms were used. The pulse was incident on the photoanode side of the cell and its intensity was controlled to keep the increment of the voltage below 10 mV. A white bias light, also incident on the same side of the cell, was supplied by light-emitting diodes. Usually, transients were measured at different white-light bias intensities ranging from 150% to 0.1% sun regulated by the applied voltage on the diodes.

  

NANO MICRO small

*Preparation of mesoscopic $TiO_2$ films and fabrication of DSCs:* The mesoscopic $TiO_2$ films used as photoanodes consisted of double layers of $TiO_2$ (6-μm thick transparent layer of 20-nm $TiO_2$ anatase nanoparticles and 4 μm thick scattering layer of 400 nm anatase $TiO_2$ particles). The detailed method of $TiO_2$ film preparation, device fabrication, and the photocurrent–voltage measurements was reported in our earlier publications.[6a,27] The double-layer films were heated to 520 °C and sintered for 30 min, then cooled to ≈80 °C and immersed into the dye (K77) solution containing 300 μM of K77 in acetonitrile and tertbutyl alcohol (volume ratio: 1:1) at room temperature for 16 h. If desired, 300 μM PPA co-adsorbent was introduced into the above dye solution. Dye-coated double-layer films were assembled and sealed with 35-μm-thick Bynel hot-melt rings (DuPont) to the counter electrodes. The latter employed FTO glass with a small amount of Pt catalyst deposited from 0.005 M hexachloroplatinic acid solution in isopropyl alcohol and subsequent heating at 400 °C for 15 min. The electrolyte was injected into the interelectrode space from the counter electrode side through a predrilled hole that was subsequently sealed with a Bynel sheet and a thin glass slide cover by heating. The IL electrolyte contained 0.2 M iodine, 0.1 M GuNCS, and 0.5 M NMB and a mixture of PMII and $EMIB(CN)_4$. For the stability testing, an electrolyte coded Z655 was employed containing 0.2 M iodine, 0.1 M GuNCS, and 0.5 M NBB the PMII/$EMIB(CN)_4$ volume ratio being 65/35.

*Photocurrent–voltage measurements*: The light source for the photocurrent–voltage (*I--V*) measurement was a 450 W xenon lamp (Oriel, USA), simulating AM 1.5 solar light. The incident light intensity was calibrated with a standard Si solar cell. The spectral output of the lamp was matched precisely to the standard global AM 1.5 solar spectrum in the region of 350–750 nm (mismatch $< 2\%$) by the aid of a Schott K113 Tempax sunlight filter (Präzisions Glas & Optik GmbH, Germany). Various irradiance intensities (from 0.01–1.0 sun) were provided with neutral wire-mesh attenuators. The current–voltage curves were obtained by measuring the photocurrent of the cells using a Keithley model 2400 digital source meter (Keithley, USA) under an applied external potential scan. The current and voltage transient measurements employed the same system. The measurement of incident photon-to-current conversion efficiency (IPCE) was recorded by a data-collecting system as a function of excitation wavelength. The incident light from a 300 W xenon lamp (ILC Technology, USA) was focused through a Gemini-180 double monochromator (Jobin Yvon Ltd., UK) onto the cell under test. No white llght bias was applied and the dc photocurrents were in a domain where their response to light intensity was linear.

*Stability test*: Hermetically sealed cells were used to check the long-term stability at 80 °C in darkness or under visible-light soaking at 60 °C. The light-soaking experiments employed a polymer film of 50-μm thickness (Preservation Equipment Ltd, UK), eliminating UV light. Cells were exposed at open circuit to a Suntest CPS lamp (ATLAS GmbH, 100 mW cm$^{-2}$, 60 °C) over a period of 1000 h. The cells were taken out at regular intervals to record the photocurrent–voltage curve.

## Acknowledgements

*The Swiss Science Foundation supports the present work. We thank P. Compte for the preparation of $TiO_2$ paste, Dr. A. McEvoy for discussion, Dr. T. Koyinagi (CCIC, Japan) for a free sample of the 400-nm light-scattering particles, and Prof. H. Willner (University of Wuppertal, Germany) and the Merck KGaA company (Darmstadt, Germany) for a sample of $EMIB(CN)_4$ ionic liquid.*

[1] B. O'Regan, M. Grätzel, *Nature* **1991**, *353*, 737.
[2] M. Grätzel, *Nature* **2001**, *414*, 338.
[3] A. Hagfeldt, M. Grätzel, *Chem. Rev.* **1995**, *95*, 49.
[4] J. N. Clifford, E. Palomares, M. K. Nazeeruddin, M. Grätzel, J. Nelson, X. Li, N. J. Long, J. R. Durrant, *J. Am. Chem. Soc.* **2004**, *126*, 5225.
[5] L. Schmidt-Mende, J. E. Kroeze, J. R. Durrant, M. K. Nazeeruddin, M. Grätzel, *Nano Lett.* **2005**, *5*, 1315.
[6] a) D. Kuang, S. Ito, B. Wenger, C. Klein, J. E. Moser, R. Humphry-Baker, S. M. Zakeerudddin, M. Grätzel, *J. Am. Chem. Soc.* **2006**, *128*, 4146; b) D. Kuang, C. Klein, H. J. Snaith, J. E. Moser, R. Humphry-Baker, P. Comte, S. M. Zakeeruddin, M. Grätzel, *Nano Lett.* **2006**, *6*, 769; c) D. Kuang, C. Klein, S. Ito, J. E. Moser, R. Humphry-Baker, S. M. Zakeeruddin, M. Grätzel, *Adv. Funct. Mater.* **2007**, *17*, 154–160; d) D. Kuang, C. Klein, S. Ito, J. E. Moser, R. Humphry-Baker, N. Evans, F. Duriaux, C. Grätzel, S. M. Zakeeruddin, M. Grätzel, *Adv. Mater.* **2007**, *19*, 1133; e) P. Wang, C. Klein, R. Humphry-Baker, S. M. Zakeeruddin, M. Grätzel, *J. Am. Chem. Soc.* **2005**, *127*, 808; f) V. Aranyos, J. Hjelm, A. Hagfeldt, H. Grennberg, *Dalton Trans.* **2003**, 1280.
[7] a) M. Grätzel, *Chem. Lett.* **2005**, *34*, 8–13; b) M. Grätzel, *Inorg. Chem.* **2005**, *44*, 6841; c) M. K. Nazeeruddin, P. Pechy, T. Renouard, S. M. Zakeeruddin, R. Humphry-Baker, P. Liska, L. Cevey, E. Costa, V. Shklover, L. Spiccia, G. B. Deacon, C. A. Bignozzi, M. Grätzel, *J. Am. Chem. Soc.* **2001**, *123*, 1613.
[8] a) Y. Chiba, A. Islam, R. Komiya, N. Koide, L. Han, *Appl. Phys. Lett.* **2006**, *88*, 223505; b) Z. S. Wang, T. Yamaguchi, H. Sugihara, H. Arakawa, *Langmuir* **2005**, *21*, 4272.
[9] P. Wang, S. M. Zakeeruddin, J. E. Moser, M. K. Nazeeruddin, T. Sekiguchi, M. Grätzel, *Nat. Mater.* **2003**, *2*, 402.
[10] C. Y. Chen, S. J. Wu, C. G. Wu, J. G. Chen, K. C. Ho, *Angew. Chem.* **2006**, *118*, 5954; *Angew. Chem. Int. Ed.* **2006**, *45*, 5822.
[11] D. Kuang, P. Wang, S. Ito, S. M. Zakeeruddin, M. Grätzel, *J. Am. Chem. Soc.* **2006**, *128*, 7732.
[12] a) P. Wasserscheid, T. Welton, *Ionic Liquids in Synthesis*, Wiley-VCH, Weinheim, Germany, **2002**; b) R. D. Dogers, K. R. Seddon, *Science* **2003**, *302*, 792; c) T. Welton, *Chem. Rev.* **1999**, *99*, 2071.
[13] a) J. Dupont, R. R. de Souza, P. A. Z. Suarez, *Chem. Rev.* **2002**, *102*, 3667; b) W. Xu, C. A. Angell, *Science* **2003**, *302*, 422; c) M. Antonietti, D. Kuang, B. Smarsly, Y. Zhou, *Angew. Chem.* **2004**, *116*, 5096; *Angew. Chem. Int. Ed.* **2004**, *43*, 4988.
[14] a) M. Yoshizawa-Fujita, D. R. MacFarlane, R. C. Howlett, M. Forsyth, *Electrochem. Commun.* **2006**, *8*, 445; b) H. Ohno, *Electrochemical Aspects of Ionic Liquids*, Wiley, New York, **2005**.
[15] a) W. Kubo, T. Kitamura, K. Hanabusa, Y. Wada, S. Yanagida, *Chem. Commun.* **2002**, 374; b) R. Kawano, H. Matsui, C. Matsuyama, A. Sato, M. A. B. H. Susan, N. Tanabe, M. Watanabe, *J. Photochem. Photobiol. A* **2004**, *164*, 87; c) H. Matsumoto, T. Matsuda, T. Tsuda, R. Hagiwara, Y. Ito, Y. Miyazaki, *Chem. Lett.* **2001**, 26; d) F. Mazille, Z. Fei, D. B. Kuang, D. Zhao, S. M. Zakeeruddin, M. Grätzel, P. J. Dyson, *Inorg. Chem.* **2006**, *45*, 1585.
[16] P. Bonhôte, A. P. Dias, M. Armand, N. Papageorgiou, K. Kalyanasundaram, M. Grätzel, *Inorg. Chem.* **1996**, *35*, 1168.

  

[17] P. Wang, B. Wenger, R. Humphry-Baker, J. E. Moser, J. Teuscher, W. Kantlehner, J. Mezger, E. V. Stoyanov, S. M. Zakeeruddin, M. Grätzel, *J. Am. Chem. Soc.* **2005**, *127*, 6850.
[18] G. Rothenberger, J. Moser, M. Grätzel, N. Serpone, D. K. Sharma, *J. Am. Chem. Soc.* **1985**, *107*, 8054.
[19] J. E. Moser, M. Grätzel, *Chem. Phys.* **1993**, *176*, 493.
[20] S. A. Haque, Y. Tachibana, R. L. Willis, J. E. Moser, M. Grätzel, D. R. Klug, J. R. Durrant, *J. Phys. Chem. B* **2000**, *104*, 538.
[21] G. Grampp, D. Kattnig, B. Mladenova, *Spectrochim. Acta Part A* **2006**, *63*, 821.
[22] Q. Wang, S. M. Zakeeruddin, M. K. Nazeeruddin, R. Humphry-Baker, M. Grätzel, *J. Am. Chem. Soc.* **2006**, *128*, 4446.
[23] S. Pelet, J. E. Moser, M. Grätzel, *J. Phys. Chem. B* **2000**, *104*, 1791.
[24] A. J. Bard, L. R. Faulkner, *Electrochemical Methods: Fundamentals and Applications*, 2nd ed., Wiley-VCH, Weinheim, Germany, **2001**.
[25] a) J. Bisquert, *J. Phys. Chem. B* **2002**, *106*, 325; b) J. Bisquert, *Phys. Chem. Chem. Phys.* **2003**, *5*, 5360; c) J. van de Lagematt, N. G. Park, A. J. Frank, *J. Phys. Chem. B* **2000**, *104*, 2044; d) J. Bisquert, A. Zaban, M. Greenshtein, I. Mora-Sero, *J. Am. Chem. Soc.* **2004**, *126*, 13550; e) R. Kern, R. Sastrawan, J. Ferber, R. Stangl, J. Luther, *Electrochim. Acta* **2002**, *47*, 4213; f) Q. Wang, J. E. Moser, M. Grätzel, *J. Phys. Chem. B* **2005**, *109*, 14945.
[26] a) E. Bernhardt, G. Henkel, H. Willner, *Z. Anorg. Allg. Chem.* **2000**, *626*, 560; b) E. Brnhardt, M. Finze, H. Willner, *Z. Anorg. Allg. Chem.* **2003**, *629*, 1229.
[27] C. J. Barbé, F. Arendse, P. Comte, M. Jirousek, F. Lenzmann, V. Shklover, M. Grätzel, *J. Am. Ceram. Soc.* **1997**, *80*, 3157.

Received: March 22, 2007
Revised: September 5, 2007
Published online on November 20, 2007

  